Oxygen vacancies on $CuGa_2$ catalysts Enhances CO_2 Reduction to CO

Jiangfeng Mou [a], Jin Hu [a,*], Tianyou Chen [a,c*], Kaizhao Wang[a], Kaijun Wang [a] ,WeiJun Zhang [a], Shuai Wu [b], Jin Shi [b], Pengchong Zhao [b].

a. College of Materials Science and Engineering, Kunming University of Science and Technology, 121 Street, Wenchang Road 68, Kunming 650093, China

b. State Key Laboratory of Complex Nonferrous Metal Resources Clean Utilization, College of Metallurgy and Energy Engineering, Kunming University of Science and Technology, 121 Street, Wenchang Road 68, Kunming 650093, China

c. Engineering Training Center, Kunming University of Science and Technology, Kunming 650093, China

* Corresponding author: hujin@kmust.edu.cn (Jin Hu); 20230152@kust.edu.cn (Tianyou Chen)

E-mail address: hujin@kmust.edu.cn (Jin Hu); 20230152@kust.edu.cn (Tianyou Chen)

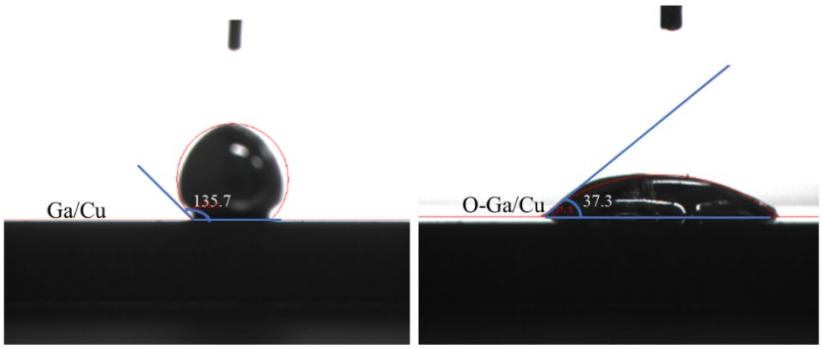

Figure. S1. the wetting angles of Ga/Cu and O-Ga/Cu.

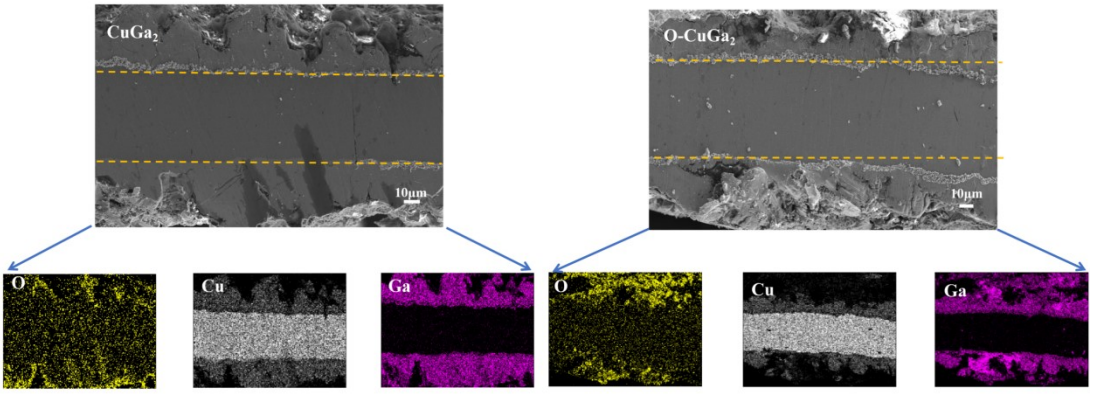

Figure. S2. Cross-sectional SEM maps and EDS elemental distribution of $CuGa_2$ and O-$CuGa_2$

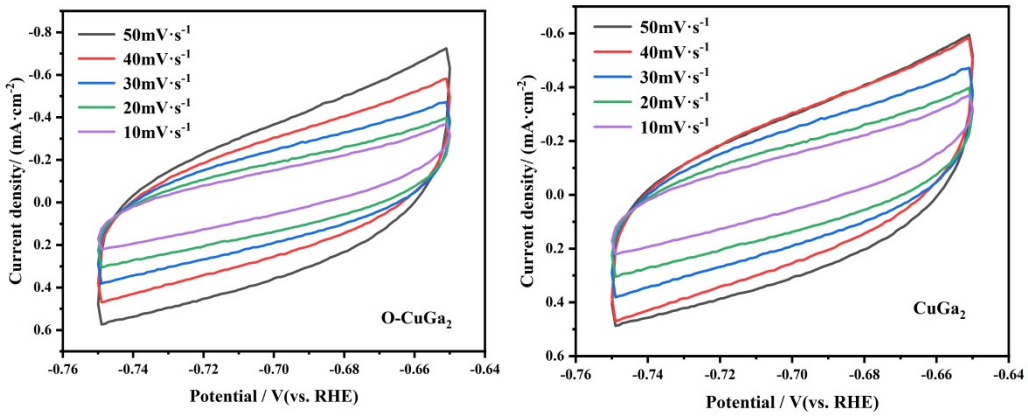

Figure.S3. Cyclic voltammograms of $CuGa_2$ and O-$CuGa_2$ at different potential scan rates under different conditions.

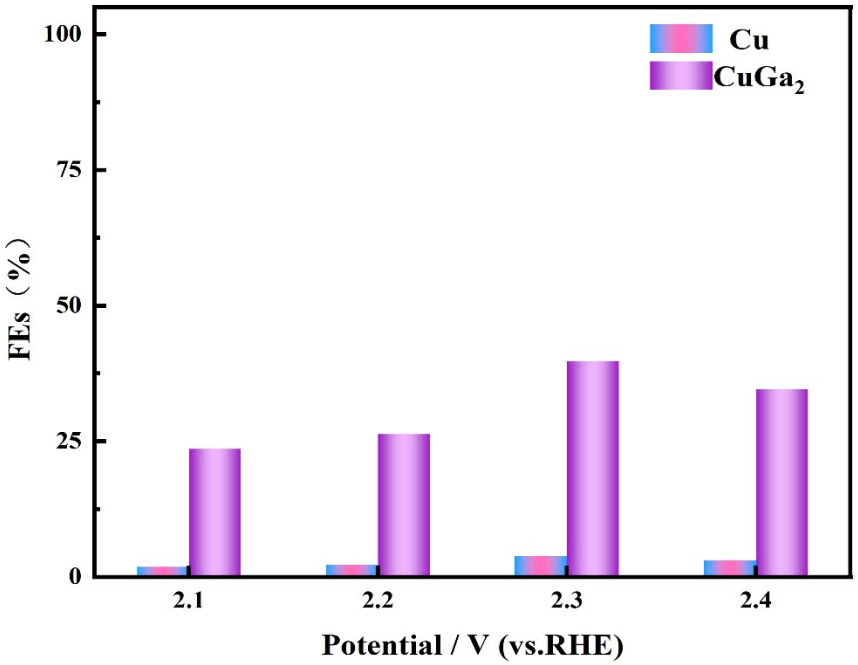

Figure . S4 Faraday efficiency plots for Cu and $CuGa_2$

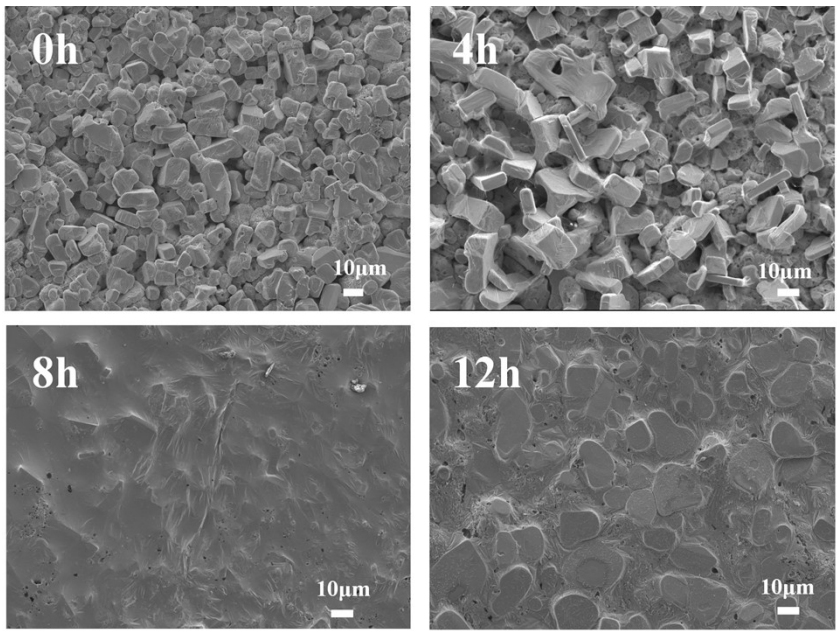

Figure. S5 SEM characterisation of O-CuGa2 electrodes prepared from O-Ga with different oxidation times.

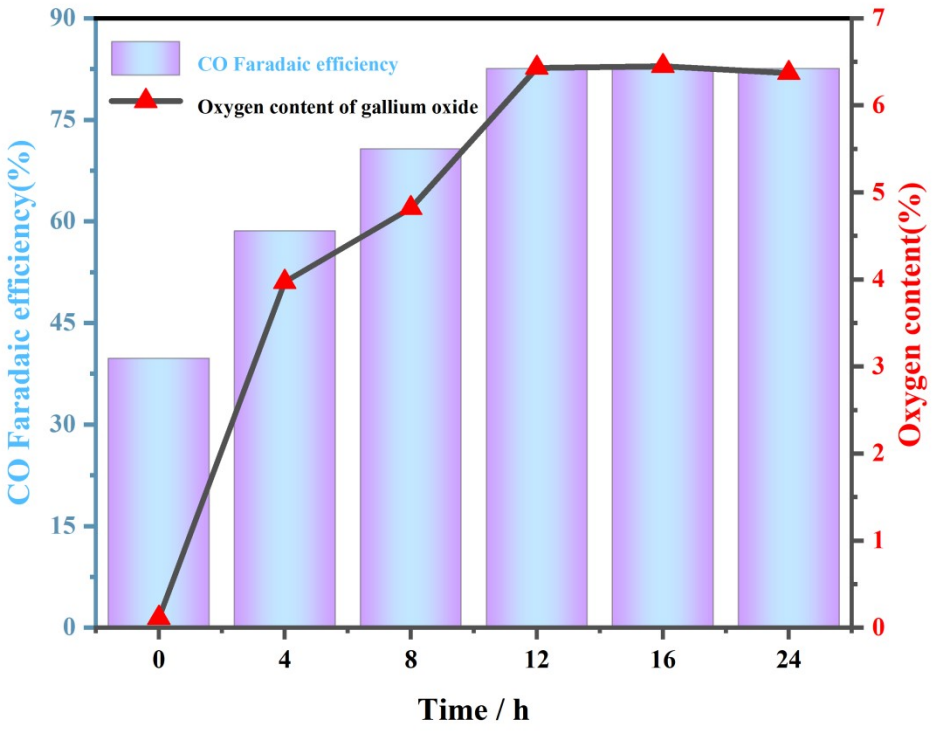

Figure. S6, Faraday efficiency plot of O-$CuGa_2$ catalysts with different oxygen contents

Table1. Rs and Rct of $CuGa_2$ and O-$CuGa_2$

Cathode	Rs（Ω）	Rct（Ω）
$CuGa_2$	4.1	14.5
O-$CuGa_2$	2.7	10.1

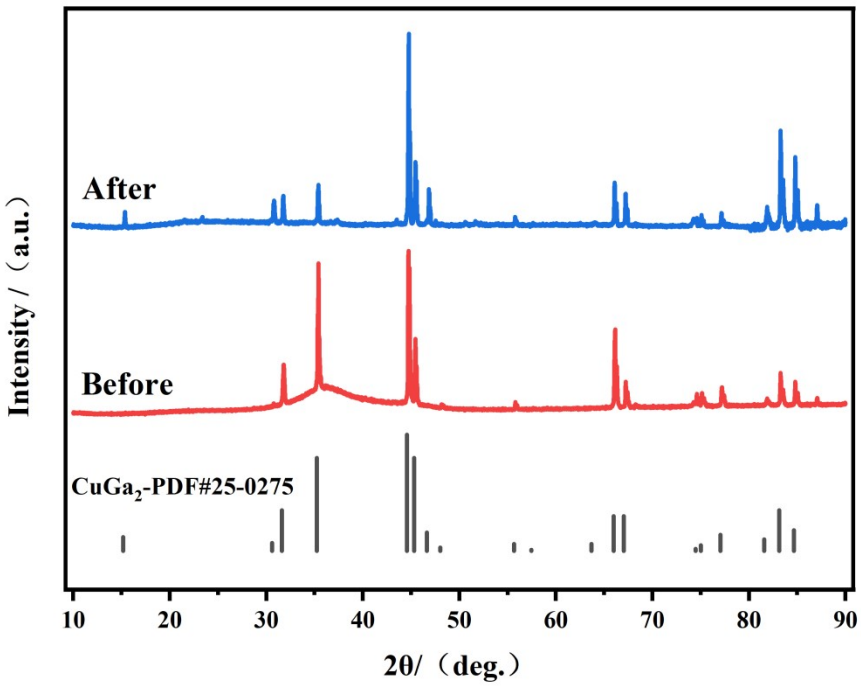

Figure. S7, XRD of the O-$CuGa_2$ electrode before and after the reaction.

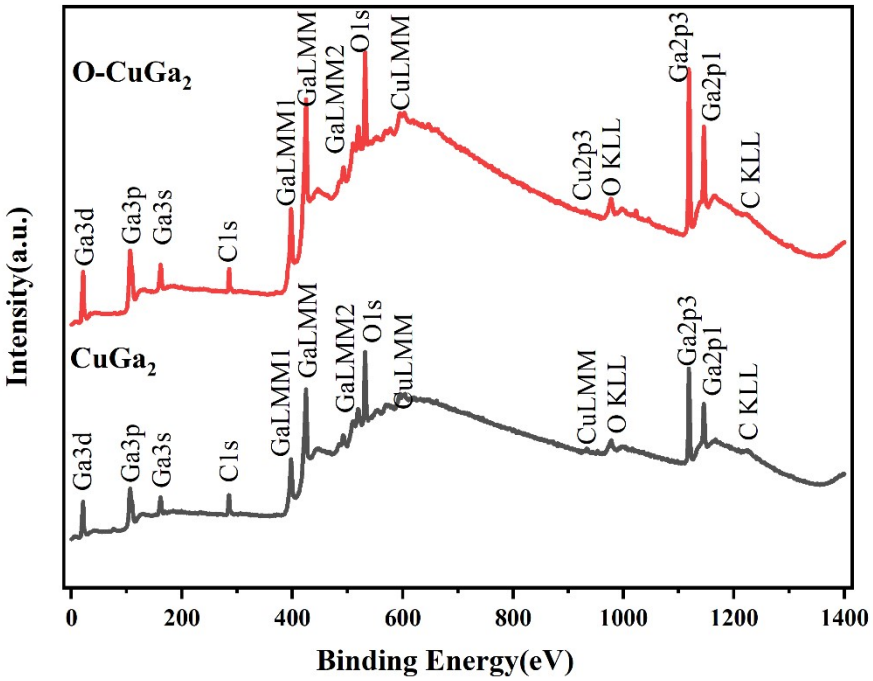

Figure .S8 XPS spectra of $CuGa_2$ and O-$CuGa_2$

Table S2. Peak summary of the high resolution XPS analysis

Region	Species	Binding energies (eV)	FWHM ($CuGa_2$)	FWHM (O-$CuGa_2$)	Area rations（Cu Ga_2）	Area rations（O-$CuGa_2$）
C 1s	C-C	284.8	1.39	1.43	100%	100%
O 1s	Ga-O	530.81	1.48	1.48	49.1%	34.3%
	O_V	531.7	1.53	1.75	30.0%	54.5%
	H_2O_{ads}	532.45	2.11	3.09	20.9%	11.2%
Ga3d	Ga^0	18.0	1.09	0.98	18%	11%
	Ga_2O_3	20.4	1.64	1.88	82%	89%
Cu2p	Cu	932.9	2.15	2.02	79.4%	75.7%
	Cu^{2+}	952.5	3.08	2.44	20.6%	24.3%

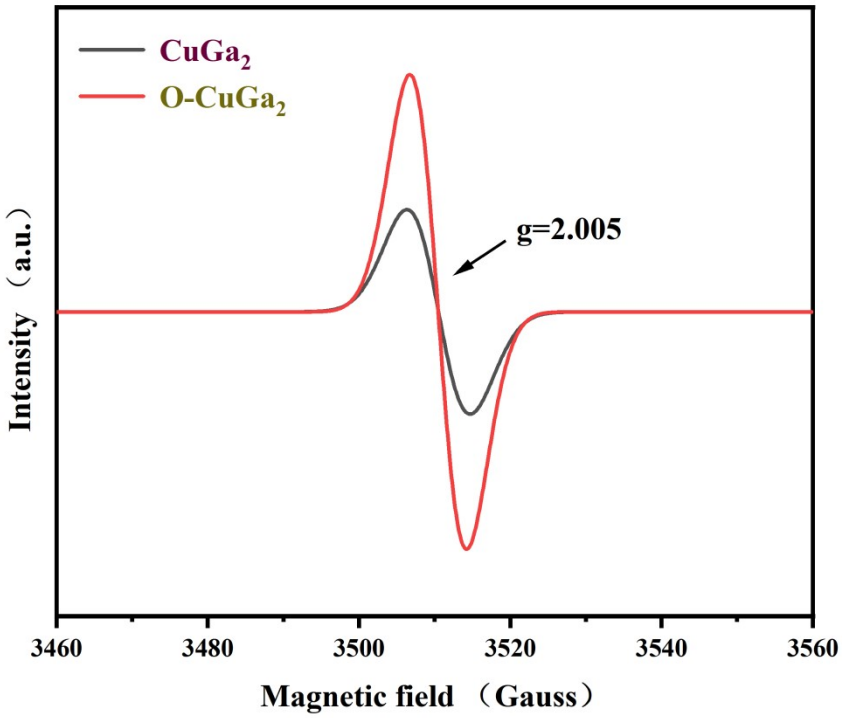

Figure. S9 EPR tests of $CuGa_2$ and O-$CuGa_2$.

Density functional theory (DFT) calculations.

The density functional theory computations were carried out by the CASTEP code, employing the ultrasoft pseudopotential [1–3]. The exchange correlation potential was represented by the Perdew-Burke-Ernzerhof (PBE) functional within the generalized gradient approximation (GGA)[4]. The Cu(111) and $CuGa_2$ (102) surface with five atomic layers was established. Periodic boundary conditions were employed along x and y directions with a vacuum region of 20 Å. The cutoff energy for the plane-wave-basis expansion is set to be 450 eV, and the convergence tolerances of energy, force and maximum displacement are set to 2.0×10^{-5} eV/atom, 5.0×10^{-2} eV/Å and 2.0×10^{-3} Å, respectively. The *k*-points grid sampling of Monkhorst-Pack scheme was set at 2×2×1. Meanwhile, the DFT-D correction method is used to describe the

long-range van der Waals interaction[5]. To calculate the d-band center, $\frac{\int N(\varepsilon)\varepsilon d\varepsilon}{\int N(\varepsilon)d\varepsilon}$ was conducted from 0 to −10.0 eV, where N(ε) is the density of states.

References:

1 G. Kresse and D. Joubert, *Phys. Rev. B*, 1999, **59**, 1758–1775.

2 G. Kresse and J. Furthmüller, *Computational Materials Science*, 1996, **6**, 15–50.

3 G. Kresse and J. Furthmüller, *Phys. Rev. B*, 1996, **54**, 11169–11186.

4 J. P. Perdew, K. Burke and M. Ernzerhof, *Phys. Rev. Lett.*, 1996, **77**, 3865–3868.

5 S. Grimme, J. Antony, S. Ehrlich and H. Krieg, *The Journal of Chemical Physics*, 2010, **132**, 154104.